

## Measuring Ensemble-Averaged Surface-Enhanced Raman Scattering in the Hotspots of Colloidal Nanoparticle Dimers and Trimers

Gang Chen, Yong Wang, Miaoxin Yang, Jun Xu, Sook Jin Goh, Ming Pan, and Hongyu Chen\*

Division of Chemistry and Biological Chemistry, Nanyang Technological University, Singapore 637371

Received October 25, 2009; E-mail: hongyuchen@ntu.edu.sg

The Raman signal intensity of molecules is greatly enhanced on a metal surface.<sup>1</sup> This effect, known as surface-enhanced Raman scattering (SERS), is exceptionally strong in the gap between plasmon-coupled metal nanoparticles (NPs).<sup>2</sup> Measuring the enhancement factor (EF) at such SERS “hotspots” is of great significance for both fundamental studies and practical applications. A key challenge in this field is to evaluate the EF from a statistically significant number of SERS hotspots in which the analyte molecules experience similar chemical and physical environments: (a) the NPs constituting the hotspots have uniform size and morphology, if not precisely known; and (c) the nanoclusters have similar structures with long-term stability. However, the current nanofabrication methods are still far from ideal in achieving these controls.

The SERS EF from hotspots has mostly been studied at the single-nanocluster level,<sup>3</sup> which is advantageous for the understanding of the individual behavior of a molecule or a nanocluster. Typical studies have prepared the nanoclusters by random aggregation of metal NPs, which were functionalized with either a single analyte<sup>3a–f</sup> or a monolayer of analytes.<sup>3g,h</sup> Because of the nonuniformity and the scarcity of the desired nanostructures, it is a challenge to correlate a SERS signal with the exact nanostructure from which it originates. Furthermore, the EF strongly depends on the specific hotspot under investigation, making it difficult to compare the results for different nanoclusters. On the other hand, ensemble-averaged studies reveal the collective behavior of SERS hotspots, which is more reproducible and controllable. However, such studies require the fabrication of highly uniform nanostructures and to date have been restricted to noncolloidal systems with extended surface-plasmon coupling, e.g., between NPs and a metallic film<sup>4</sup> or among NPs in a two-dimensional lattice.<sup>5</sup>

Here we report the measurement of the ensemble-averaged SERS EF from spatially isolated colloidal nanoclusters (Figure 1). This was made possible by advances in precise nanofabrication: uniform-sized Au@Ag core-shell NPs, each coated with a monolayer of SERS analytes, were aggregated and then protected by a polymer shell; separation of the resulting nanoclusters led to samples enriched in dimers (85%) and trimers (70%). The structural uniformity of the hotspots therein reduced the ambiguities in calculating and interpreting the respective EFs.

High-purity separation of AuNP dimers and trimers by differential centrifugation, where shells of polystyrene-*block*-poly(acrylic acid) (PSPAA) were used to enclose and protect the nanoclusters, has been reported previously.<sup>6a,b</sup> However, the AuNPs used in those reports were too small (15 nm) to give reliable SERS signals. To improve the SERS sensitivity, one has to use either AgNPs or large AuNPs (>40 nm). As a 25% increase in diameter doubles the NP volume, controlling the monodispersity of the NPs is critical for effective separation of the nanoclusters.<sup>6</sup> Moreover, since our differential centrifugation method used a high-density CsCl solution (1.9 g cm<sup>-3</sup>) to distinguish nanoclusters of different

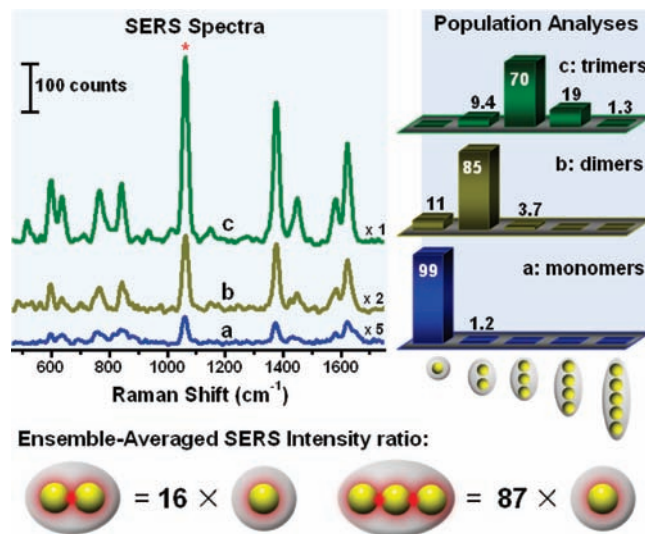


**Figure 1.** SERS spectra of the samples enriched with (a) monomers, (b) dimers, and (c) trimers of Au@Ag NPs ( $d = 20$  nm; excitation: 785 nm at 290 mW; insets: the histograms of these samples). The schematics in the lower panel show the SERS intensity ratio of the nanoclusters.

sizes, use of large and heavy AuNPs was not desirable. Hence, acquiring monodispersed AgNPs became the only option. While several syntheses of AgNPs are known,<sup>7</sup> the size distributions were not ideal for our purpose. In this study, to prepare highly monodisperse Au@Ag core-shell NPs ( $d_{\text{Au@Ag}} = 20.5 \pm 1.5$  nm; Figure 2a), we used a method wherein AgNO<sub>3</sub> was reduced by ascorbic acid using AuNPs (3–4 nm) as the seeds and sodium citrate as the capping agent. Avoiding strong ligands allowed the NP surface to be easily exchanged with SERS-active ligands. The absorption peak of the Au@Ag NPs (400 nm)<sup>8</sup> was similar to that of 20 nm AgNPs, suggesting that the Au cores did not contribute to the plasmon resonance of the overall NPs.<sup>9</sup>

To prepare the nanoclusters, the citrate-stabilized Au@Ag NPs were incubated with excess analyte (2-naphthalenethiol, **1**) in DMF to fully exchange the surface ligands and form a monolayer; NaCl was then added (0.33 mM) to induce NP aggregation, and the resulting nanoclusters were encapsulated in PSPAA.<sup>6b</sup> Transmission electron microscopy (TEM) characterization showed that a typical as-synthesized sample consisted of 41% monomers, 32% dimers, 16% trimers, and 8% tetramers (based on the number of Au@Ag NPs).<sup>8</sup> The control sample of monomers was prepared by incubating the Au@Ag NPs with **1** followed by PSPAA encapsulation (Figure 2a).<sup>10</sup> In comparison with the monomers, the Au@Ag NPs in the NaCl-treated samples appeared somewhat etched and thus became less uniform ( $d_{\text{Au@Ag}} = 20.3 \pm 3.5$  nm). However, use of another salt, such as NaNO<sub>3</sub>, NaOAc, Na<sub>2</sub>SO<sub>4</sub>, or Na<sub>3</sub>PO<sub>4</sub>, did not resolve the problem. While it was unfortunate that the aggregation step partially compromised the size monodispersity of the NPs, the differential

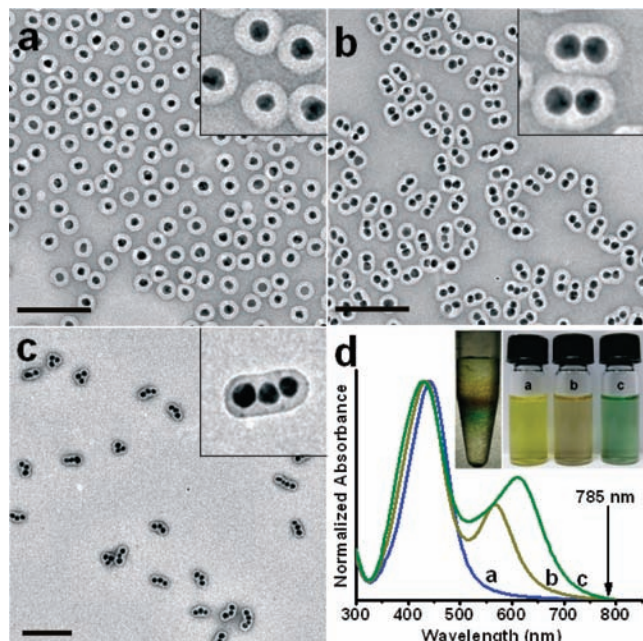


**Figure 2.** (a–c) TEM images and (d) UV–vis spectra of the samples enriched with Au@Ag monomers (a), dimers (b), and trimers (c). Though often in a bent conformation, the trimers mostly contained only two hotspots. Clear gaps existed within the nanoclusters, and no fusion was observed. The inset in (d) shows a typical outcome of the differential centrifugation, where monomers, dimers, and trimers were enriched in distinct yellow, brown, and green bands, respectively. Scale bars: 200 nm.

centrifugation<sup>6b</sup> of the nanoclusters still gave reasonable results (Figure 2). Multiple separations of products from scaled-up colloidal syntheses led to a sufficient quantity of dimers and trimers (85.1 and 70.3%, respectively; statistics based on at least 800 clusters) with slightly reduced purity. The UV–vis spectra of the dimers and trimers (Figure 2d) showed clear transverse plasmon bands, indicating strong coupling within the nanoclusters. A 785 nm laser was used for the SERS study to avoid the different absorbance of the colloidal nanoclusters (Figure 2d). TEM images showed that the NPs did not fuse together, and the gap distance was relatively uniform with an average of 0.8 nm.<sup>8</sup>

While the statistics based on the TEM images gave the relative abundance of the nanoclusters in a particular sample, comparing the concentrations of different samples was not trivial, particularly after the aggregation and loss of NPs during the processing steps. It was noticed that when identical samples of Au@Ag NPs underwent different degrees of aggregation, there existed an isosbestic point (325 nm) in the corresponding UV–vis spectra (Figure S6 in the Supporting Information).<sup>8</sup> On the basis of this aggregation-independent absorbance, the relative concentrations of Au@Ag NPs in the samples can be obtained.<sup>8</sup> Combining the relative SERS intensities allowed the averaged intensities of dimers ( $I_{2NP}$ ) and trimers ( $I_{3NP}$ ) at 1064 cm<sup>-1</sup> (Figure 1) to be calculated by solution of multivariate equations in which  $I_{2NP}$  and  $I_{3NP}$  were set as the unknowns and the intensities of tetramers and pentamers were assumed to be linearly proportional to the number of hotspots therein ( $I_{nNP} = a(n - 1)(I_{3NP}/2)$ , where  $a$  is a coefficient whose value was estimated to be 2 on the basis of our measurements of a sample enriched in large nanoclusters).<sup>8</sup>

The results were  $I_{2NP} = 16I_{1NP}$  (i.e., 8 times as strong per NP) and  $I_{3NP} = 87I_{1NP}$ . If the hotspot is assumed to constitute 1/100 of the total NP surface (i.e., 13 nm<sup>2</sup>), then each dimeric hotspot would be 700 times as strong as a monomer and each trimeric hotspot 2100 times as strong per unit area.<sup>8</sup> If 130 nm<sup>2</sup> of hotspot area is assumed, then the values would be 70 and 210, respectively. It should be noted that these calculations did not rely on the absolute concentrations of the

NPs and thus avoided the related assumptions. In our system, ligand **1** forms a monolayer on the Au@Ag NPs. Control experiments showed that three independent syntheses of the monomer samples gave SERS intensities with less than 5% standard deviation, demonstrating the reproducibility of the ligand monolayer. Comparing the SERS intensity of a monomer sample with that of free **1** in CHCl<sub>3</sub> gave an ensemble-averaged EF of  $1.3 \times 10^3$ . This estimate depends on the actual ligand density and the total surface area of the Au@Ag NPs, both of which are difficult to measure precisely.<sup>8</sup>

Hence, the ensemble-averaged EFs at the hotspots of the dimers and trimers ( $d_{Au@Ag} = 20$  nm) should be in the range of  $10^5$ – $10^7$ . The uncertainty also stems from the poorly defined hotspot area and the lack of understanding of the EF distribution within the hotspots. The small EF observed could be attributed to the non-resonance-Raman signal of **1**, the weak absorbance of the nanoclusters at 785 nm, and the random alignment of the nanoclusters in the colloid with respect to the incident light. Therefore, under optimal conditions, the EF of the “hottest” molecule may exceed our estimates by several orders of magnitude.

Despite these uncertainties, the relative intensity ratios of the nanoclusters ( $I_{2NP} = 16I_{1NP}$  and  $I_{3NP} = 87I_{1NP}$ ) involve few assumptions and are thus more reliable. The formation of the monolayer of **1** on each NP before aggregation reduces the ambiguity of analyte location in the hotspots and gives rise to uniform gap distances between NPs. Enclosed by the polymer shells, the nanoclusters are free from transient aggregation and the surface ligands (analytes) are immune to exchange and dissociation. The ensemble-averaged measurement of colloidal hotspots provides unique advantages in averaging out the “blinking” of single-molecule SERS and minimizing the photodamage of analytes.

**Acknowledgment.** The authors thank the Ministry of Education, Singapore, for financial support (ARC 27/07 and 13/09).

**Supporting Information Available:** Details of experimental procedures, calculations, and large TEM images. This material is available free of charge via the Internet at <http://pubs.acs.org>.

## References

- (1) Moskovits, M. *Rev. Mod. Phys.* **1985**, *57*, 783.
- (2) (a) Xu, H. X.; Bjerneld, E. J.; Kall, M.; Borjesson, L. *Phys. Rev. Lett.* **1999**, *83*, 4357. (b) Hao, E.; Schatz, G. C. *J. Chem. Phys.* **2004**, *120*, 357. (c) Camden, J. P.; Dieringer, J. A.; Zhao, J.; Van Duyne, R. P. *Acc. Chem. Res.* **2008**, *41*, 1653.
- (3) (a) Nie, S. M.; Emery, S. R. *Science* **1997**, *275*, 1102. (b) Kneipp, K.; Wang, Y.; Kneipp, H.; Perelman, L. T.; Itzkan, I.; Dasari, R.; Feld, M. S. *Phys. Rev. Lett.* **1997**, *78*, 1667. (c) Michaels, A. M.; Nirmal, M.; Brus, L. E. *J. Am. Chem. Soc.* **1999**, *121*, 9932. (d) Camden, J. P.; Dieringer, J. A.; Wang, Y. M.; Masiello, D. J.; Marks, L. D.; Schatz, G. C.; Van Duyne, R. P. *J. Am. Chem. Soc.* **2008**, *130*, 12616. (e) Qian, X. M.; Nie, S. M. *Chem. Soc. Rev.* **2008**, *37*, 912. (f) Dadosh, T.; Sperling, J.; Bryant, G. W.; Breslow, R.; Shegai, T.; Dyshel, M.; Haran, G.; Bar-Joseph, I. *ACS Nano* **2009**, *3*, 1988. (g) Camargo, P. H. C.; Rycenga, M.; Au, L.; Xia, Y. N. *Angew. Chem., Int. Ed.* **2009**, *48*, 2180. (h) Li, W. Y.; Camargo, P. H. C.; Lu, X. M.; Xia, Y. N. *Nano Lett.* **2009**, *9*, 485.
- (4) Braun, G.; Lee, S. J.; Dante, M.; Nguyen, T. Q.; Moskovits, M.; Reich, N. J. *Am. Chem. Soc.* **2007**, *129*, 6378.
- (5) (a) Wang, H.; Levin, C. S.; Halas, N. J. *J. Am. Chem. Soc.* **2005**, *127*, 14992. (b) Lee, S. J.; Morrill, A. R.; Moskovits, M. *J. Am. Chem. Soc.* **2006**, *128*, 2200. (c) Braun, G.; Pavel, I.; Morrill, A. R.; Seferos, D. S.; Bazan, G. C.; Reich, N. O.; Moskovits, M. *J. Am. Chem. Soc.* **2007**, *129*, 7760.
- (6) (a) Wang, X. J.; Li, G. P.; Chen, T.; Yang, M. X.; Zhang, Z.; Wu, T.; Chen, H. *Nano Lett.* **2008**, *8*, 2643. (b) Chen, G.; Wang, Y.; Tan, L. H.; Yang, M. X.; Tan, L. S.; Chen, Y.; Chen, H. *J. Am. Chem. Soc.* **2009**, *131*, 4218. (c) Sun, X. M.; Tabakman, S. M.; Seo, W. S.; Zhang, L.; Zhang, G. Y.; Sherlock, S.; Bai, L.; Dai, H. *J. Angew. Chem., Int. Ed.* **2009**, *48*, 939.
- (7) (a) Wiley, B.; Herricks, T.; Sun, Y. G.; Xia, Y. N. *Nano Lett.* **2004**, *4*, 1733. (b) Wiley, B.; Sun, Y.; Xia, Y. N. *Acc. Chem. Res.* **2007**, *40*, 1067.
- (8) See the Supporting Information.
- (9) Xing, S.; Tan, L. H.; Chen, T.; Yang, Y.; Chen, H. *Chem. Commun.* **2009**, 1653.
- (10) (a) Chen, H.; Abraham, S.; Mendenhall, J.; Delamarre, S. C.; Smith, K.; Kim, I.; Batt, C. A. *ChemPhysChem* **2008**, *9*, 388. (b) Yang, M. X.; Chen, T.; Lau, W. S.; Wang, Y.; Tang, Q. H.; Yang, Y. H.; Chen, H. *Small* **2009**, *5*, 198. (c) Kang, Y. J.; Taton, T. A. *Angew. Chem., Int. Ed.* **2005**, *44*, 409.

JA9090885